GEOPHYSICAL RESEARCH LETTERS, VOL. 34, L18102, doi:10.1029/2007GL030030, 2007

Click Here for Full Article

Water ice permafrost on Mars: Layering structure and subsurface distribution according to HEND/Odyssey and MOLA/MGS data

I. G. Mitrofanov,[1] M. T. Zuber,[2] M. L. Litvak,[1] N. E. Demidov,[1,3] A. B. Sanin,[1] W. V. Boynton,[4] D. A. Gilichinsky,[3] D. Hamara,[4] A. S. Kozyrev,[1] R. D. Saunders,[5] D. E. Smith,[6] and V. I. Tretyakov[1]

Received 15 March 2007; revised 6 June 2007; accepted 23 July 2007; published 20 September 2007.

[1] To elucidate the nature of permafrost in the shallow subsurface of Mars, we analyze jointly neutron albedo from the High Energy Neutron Detector (HEND) on the Mars Odyssey spacecraft and near-IR (1064-nm) surface reflectance from the Mars Orbiter Laser Altimeter (MOLA) on Mars Global Surveyor. The first dataset measures the content of hydrogen (in the form of water or hydroxyl) in the soil, and the second yields the flux of absorbed solar energy by the surface. We identify a statistically–significant negative cross-correlation between these data at latitudes poleward of 40° latitude in the northern hemisphere and in the latitude band 40°–60° in the southern hemisphere, which we interpret as evidence for the presence of stable water ice under a dry equilibrium top layer (ETL). We deduce an empirical relation between near-IR reflectance and thickness of this ETL, which allows the burial depth of the water ice table to be estimated with km-scale spatial resolution. We observe no correlation between neutron and near-IR albedo within the southern hemisphere poleward of 60° latitude. While it is known from previously analyzed neutron and gamma-ray data that subsurface water ice is present within this region and is covered by a layer of dry regolith, the absence of a correlation indicates that the thickness of this layer is not controlled by an equilibrium condition between the ice table and atmosphere. **Citation:** Mitrofanov, I. G., et al. (2007), Water ice permafrost on Mars: Layering structure and subsurface distribution according to HEND/Odyssey and MOLA/MGS data, *Geophys. Res. Lett.*, *34*, L18102, doi:10.1029/2007GL030030.

1. Introduction

[2] Neutron emission from the surface of Mars is known to be produced by bombardment of galactic cosmic rays. Cosmic ray-generated high-energy neutrons are moderated down to fast, epithermal and thermal energies before escaping from the surface, and the proportions between them depend on the content of hydrogen in the soil. The primary constituent in the shallow subsurface of Mars that contains hydrogen is water: either water ice, or physically-bound water on the surface of regolith grains, or chemically-bound water in hydrated minerals. The efficiency of neutron moderation increases with increasing fraction of *H* in the bulk composition of the soil. As the fraction of *H* increases, the flux of escaping epithermal neutrons decreases, and the flux of escaping thermal neutrons increases, but the total number of escaping neutrons is not conserved because some of them can also be absorbed by *H* nuclei with creation of heavy water nuclei, *D*, and 2.2-MeV gamma-ray photons. Measurements of neutrons and 2.2-MeV gamma-rays by the instruments that comprise the Gamma Ray Spectrometer suite on the Mars Odyssey spacecraft have enabled the water content of the shallow subsurface in different regions of Mars to be estimated [*Boynton et al.*, 2002; *Mitrofanov et al.*, 2002, 2003, 2004; *Feldman et al.*, 2002; *Litvak et al.*, 2006]. Two large provinces of permafrost have been discovered poleward of 60°N and 60°S with the content of water in the soil up to 50–70 weight per cent, which means that water ice is the dominant constituent in the shallow subsurface.

[3] The northern and southern hemisphere permafrost provinces are quite distinct; they are characterized by different altitudes, ages, relief and geology. Unfortunately, analysis of orbital neutron and gamma-ray data do not in themselves permit unambiguous interpretation regarding the vertical distribution of H_2O in the subsurface, because the observed emission is produced by cosmic ray interactions that occur within the surface layer to a depth of about 1 meter. Estimation of the flux of neutrons and gamma-rays is based on solution of an integral equation, which balances the emitted outward flux with the integral over the depth *Z* from the product of *Z*-dependent functions of particle propagation and of composition [e.g., see *Mitrofanov et al.*, 2004]. However, there is the evidence in the HEND neutron data that southern hemisphere permafrost has a two-layer structure with a dry layer of about 10–20-cm thickness overlying a water-rich lower layer; in contrast, in the northern hemisphere permafrost the dry top layer has not been resolved [*Mitrofanov et al.*, 2004; *Litvak et al.*, 2006].

[4] The content of either adsorbed or chemically-bound water in the soil does not depend on heating of surface by sunlight. Minerals could be hydrated when the water vapor pressure is high, or when the minerals are subjected to aqueous conditions for some period. Water bound in a mineral matrix cannot be liberated without significant heating that changes the crystalline structure [*Bishop*, 2005]. Adsorbed water in the soil exists as multi-layers of molecules on the surface of regolith grains, and only small fraction of this water could vary as thermal and moisture conditions

[1]Institute for Space Research, Moscow, Russia.
[2]Department of Earth, Atmospheric and Planetary Sciences, Massachusetts Institute of Technology, Cambridge, Massachusetts, USA.
[3]Institute of Physical-Chemical and Biological Problems of Soil Science, Pushchino, Russia.
[4]Lunar and Planetary Laboratory, University of Arizona, Tucson, Arizona, USA.
[5]NASA Headquarters, Washington, DC, USA.
[6]Solar System Exploration Division, NASA Goddard Space Flight Center, Greenbelt, Maryland, USA.

Copyright 2007 by the American Geophysical Union.
0094-8276/07/2007GL030030$05.00

change during diurnal and seasonal cycles. These forms of water constitute a rather insignificant fraction of the soil, and can be ignored in interpretations of significant spatial variations of neutron albedo over the Martian surface. The only form of subsurface water that is significant enough, in the sense of volumetric content, to explain the observed variation observed on Mars at high latitudes, is free water ice, which is known to depend on solar heating of the surface.

[5] At both Martian poles water ice is stable in part due to low solar insolation. Equatorward of the poles stable water ice exists in the shallow regolith, but is believed to be covered by a layer of dry material [*Mellon and Jakosky*, 1995]. This layer protects the water ice either by reducing the sublimation rate of water molecules and/or by attenuating the average temperature above the ice table. The depth of the ice table could be determined by the equilibrium condition between the temperature of subsurface and the density of water vapor [*Schorghofer and Aharonson*, 2005]. However, the burial depth could be shifted out of equilibrium either due to wind erosion, or dust deposition, or change of atmospheric pressure. The burial depth could correspond to the condition of equilibrium, provided time for getting equilibrium would be much shorter than the time of any surface variations. Therefore, we may logically distinguish two cases by introducing the concept of an *equilibrium top layer* (*ETL*) for the case of equilibrium and *dry top layer* (*DTL*) for the case of non-equilibrium. The thickness of *ETL* depends mainly on the heating flux of sunlight, which is proportional to $(100 - A)$, where A is the surface albedo (in %) for sunlight. If the average temperature in the shallow subsurface is low enough for water ice to be stable, the thickness of *ETL* should be greater in areas where the solar heat flux is higher.

[6] Analysis of HEND neutron data [*Mitrofanov et al.*, 2002, 2004; *Litvak et al.*, 2006] and GRS gamma-ray data (W. V. Boynton et al., Concentration of H, Si, Cl, K, Fe, and Th in the low-latitude and midlatitude regions of Mars, submitted to *Journal of Geophysical Research*, 2007) has shown that a rather simple double layer model is supported for Martian polar permafrost regions. The model assumes a surficial dry or desiccated layer with variable thickness h that overlies an ice-bearing layer with variable ice content, ζ. According to this model, spatial variations of neutron albedo may be produced by h, ζ, or a combination of the two. In analysis of HEND data we have used both h and ζ as free-fitting parameters to obtain the best agreement between the predicted neutron flux and observations, but we were aware that neutron data taken alone are not sufficient for unambiguous determination. Additional data, or additional hypotheses are necessary to achieve a unique solution.

[7] Below we test the hypotheses that thickness of dry top layer is the major reason for the observed spatial variations of neutron emission and that this layer has the physical nature of an *ETL*. Because the thickness of the *ETL* is determined by the solar insolation, it is possible to test whether neutron albedo and surface albedo for sunlight are correlated, which is a necessary condition for this scenario to be valid.

2. Data Analysis

[8] We use radiometry data [*Sun et al.*, 2006] from the MOLA altimeter, which measures surface or atmosphere reflectance within a 2-nm bandwidth centered at 1064 nm [*Zuber et al.*, 1992; *Smith et al.*, 2001]. These observations correspond to the surface reflectivity of Mars in the near-IR and have sub-kilometer spatial resolution [*Sun et al.*, 2006]. For comparison, the HEND data for neutron albedo have much coarser spatial resolution, approximately 300 km. To jointly analyze these data sets, we utilized a $5^\circ \times 5^\circ$ (latitude $\times$ longitude) grid of surface elements for the HEND neutron data, and averaged the MOLA radometry data over the same pixels. We co-registered the neutron and near-IR albedo along 5° latitude bands (72 pixels in each band) around Mars. In such analysis we excluded the difference of solar irradiation at different latitudes. For each surface element we used albedo data for summer seasons only (Figure 1), when there is no surface condensation of atmospheric carbon dioxide. The HEND data include 4 years of observations from February 2002 until October 2006. For high northern and southern latitudes (poleward of 60°) the HEND data were used for the northern summer $L_s = [90^\circ, 180^\circ]$ and southern summer $L_s = [270^\circ, 360^\circ]$, respectively. The MOLA radiometry data were collected during the summer of the same Martian years: $L_s = [150^\circ - 165^\circ]$ for the northern hemisphere and $L_s = [330^\circ - 345^\circ]$ for the southern hemisphere, respectively.

[9] Figure 2 shows cross-correlation coefficients C between the HEND counting rate f_n of epithermal neutrons (in counts/s) and the MOLA near-IR albedo A_{1064} (in %) for 5° latitude bands over the Martian surface. We excluded regions at high polar latitudes (>80°) in the north and south, because the residual polar caps influence the surface albedo at these latitudes. The analysis requires $C > 0.325$ for statistical significance (3σ level), and with this criterion we observe no significant correlation within the broad equatorial belt *I* (40°S; 40°N). The absence of a meaningful correlation indicates that content of water in the soil within the belt *I* does not depend on the solar heating of the shallow subsurface. In this case spatial variations of neutron emission within belt *I* represent variations of either chemically-bound water in hydrated minerals, or adsorbed water in the regolith, or both. However, visual inspection shows some qualitative coincidence between the signatures of low neutron emission and high surface albedo within Arabia and Memnonia (see Figure 1): we shall apply some another technique for quantitative comparison between them elsewhere.

[10] There are two other latitude bands, which we designate as belts *II* (40°N; 80°N) and *III* (40°S; 60°S), that exhibit significant cross-correlation of neutron and near-IR albedo (f_n, A_{1064}). No cross-correlation is found in belt *IV* poleward of 60°S latitude (Figure 2). Northern belt *II* is much broader than southern belt *III*. The negative sign of the cross-correlation indicates that the increase of near-IR albedo A_{1064} is accompanied by a decrease of neutron albedo f_n. We interpret the observed cross-correlation for latitude belts *II* and *III* to indicate that the thickness of a dry layer above a table of water ice is influenced significantly by absorbed sunlight, or in another words, the top layer of dry regolith has the physical properties of an *ETL*.

[11] To test this hypothesis, we selected within belts *II* and *III* six 5°-latitude bands that exhibit the high negative correlation: (a) (50°N–55°N), (b) (60°N–65°N), (c) (70°N–75°N), (d) (55°S–60°S), (e) (50°S–55°S) and (f) (45°S–50°S) (Figure 2). We used the HEND data to estimate the best-fit parameter $h^{(*)}$, which represents the thickness of the

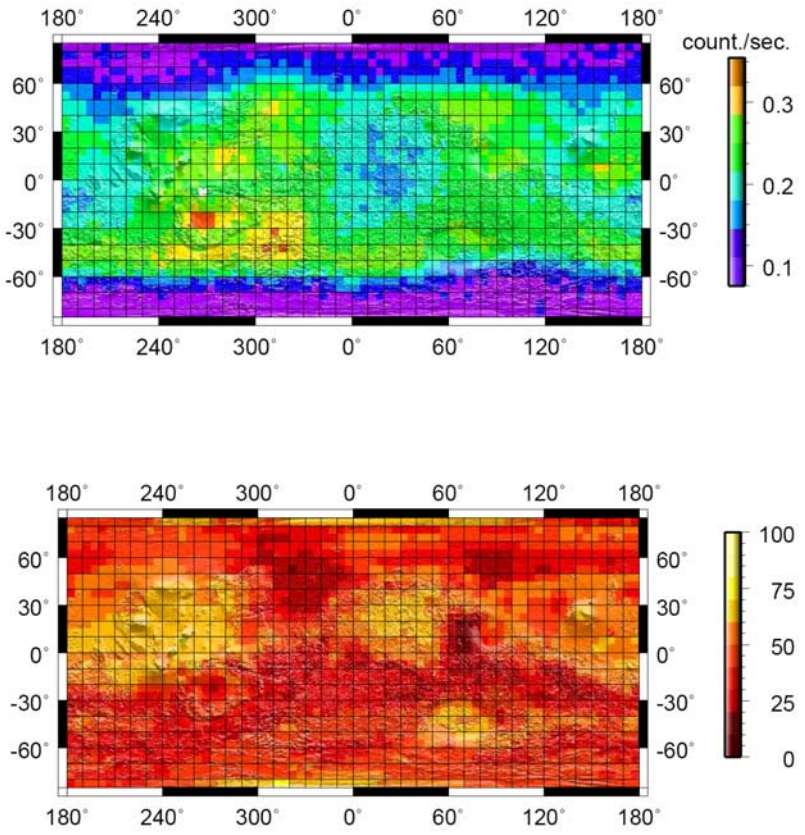

Figure 1. (top) Surface distribution of albedo of epithermal neutrons (counts/sec) for summer seasons on Mars according to HEND data from Mars Odyssey [*Mitrofanov et al.*, 2004; *Litvak et al.*, 2006]. (bottom) Surface distribution of near-IR albedo (%) for summer seasons of Mars according to MOLA radiometry observations from Mars Global Surveyor [*Sun et al.*, 2006].

dry layer, individually for each spatial element along the band, assuming the content of water in the bottom layer to be equal to the maximum value estimated within each band. We also estimated the heating by sunlight for the same surface elements within these bands. The solar heating at noon in summer (ignoring atmospheric emission estimated to be of order 4% [*Schorghofer and Aharonson*, 2005]) is proportional to $F\,(100 - A_{1064})\cos(|\varphi| - \delta) = F_0 W$, where F is flux of solar illumination, φ is latitude, and δ is the declination of the sun. The insolation parameter W (measured in %) depends on the fraction of absorbed energy $\sim(100 - A_{1064})$, and also takes into account the distance to sun and local solar elevation. We may thus define it as

$$W = \mu(100 - A_{1064}) \cdot \cos(|\varphi| - \delta), \tag{1}$$

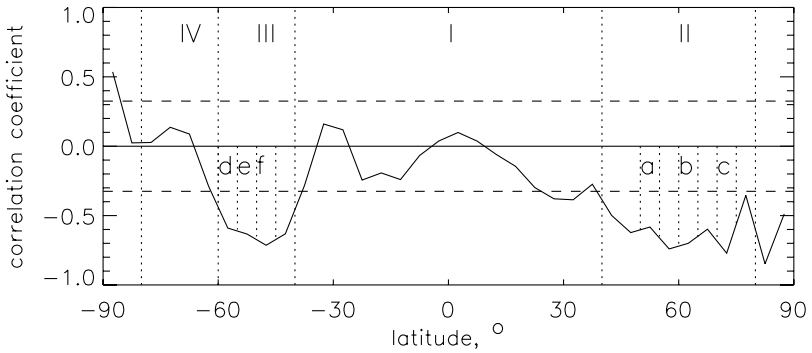

Figure 2. Correlation coefficient between neutron albedo and near-IR albedo along different latitude bands. Levels of significance are shown by the dashed line, while dotted lines separate belts of different cross-correlation. Six bands, a–f, are shown by light dotted lines, which are used for model-dependent comparison between the thickness of the top layer and the power of absorbed energy (Figure 3).

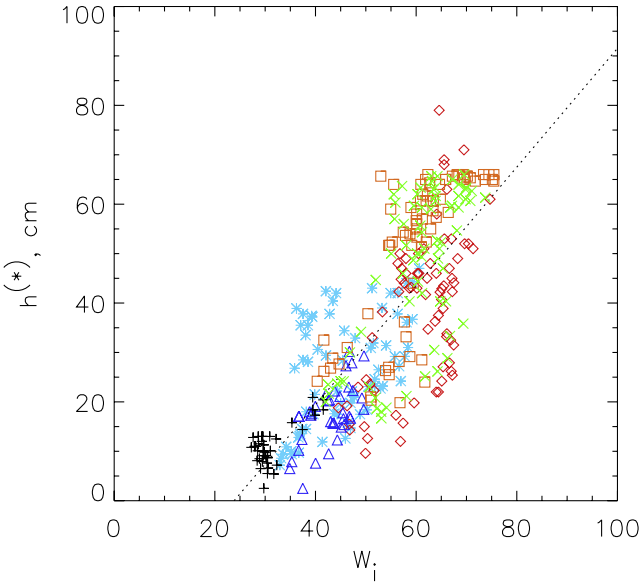

Figure 3. Values of $(h_i^{(*)}W_i)$ for six bands, a–f (Figure 2), with high correlation: band a (50°N–55°N, blue), band b (60°N–65°N, dark blue) and band c (70°N–75°N, black) in the northern hemisphere and band d (55°S–60°S, red), band e (50°S–55°S, green) and band f (45°S–50°S, orange) in the southern hemisphere. The dotted line shows a linear fit to the data (expression (2)).

with $\mu_{NS} = 0.85$ for northern summer and $\mu_{SS} = 1.2$ for southern summer. The product of flux of sunlight F_0 at the average distance of Mars' orbit and the insolation parameter W is equal to the total power absorbed by each cm^2 of a surface at noon in Martian astronomical summer.

[12] We find significant correlation between the best-fit burial depth $h^{(*)}$ and insolation parameter W with coefficients $C^{(a)} = 0.49$, $C^{(b)} = 0.64$ and $C^{(c)} = 0.64$, $C^{(d)} = 0.58$, $C^{(e)} = 0.65$ and $C^{(f)} = 0.74$, respectively for bands a–f. These results, when taken together, yield a rather strong cross-correlation $C^{(a)-(f)} = 0.80$ (Figure 3). We conclude that the observed variations of neutron emission within belts *II* and *III* can be attributed to changes in the thickness of the *ETL*, which is determined by absorbed fraction of sunlight. Using the scatter plot of points $(h^{(*)}, W)$ shown in Figure 3, we may extract a simple empirical relationship between the thickness h_{ETL} of the *ETL* above the water ice table and the insolation parameter, W, as

$$h_{ETL} = k(W - W_0), \qquad (2)$$

where $k = 1.2$ cm/% and $W_0 = 23.9\%$ corresponds to the insolation conditions, when stable water ice may exist on the surface.

[13] Figure 3 shows that the dispersion of points around this interpolation is quite large, but we may plausibly attribute the variation to physical differences between individual spatial elements, which have been ignored in our analysis so far. As one example, the water ice content could vary in the bottom layer. Alternatively, the thermal properties of soil (thermal inertia, conductivity and heat capacity) could also be quite different from pixel to pixel. Or perhaps, each spatial element may have a different slope with respect to north-south. In future study we will address these additional effects. However, our analysis establishes the main empirical relationship between the thickness of *ETL* and absorbed sunlight, which we contend is the primary controlling factor that determines the burial depth of stable water ice in latitude belts *II* and *III*.

[14] Figure 1 shows that HEND neutron data, interpreted in isolation, displays equatorward boundaries of the northern and southern permafrost provinces at latitudes of 55°–60°. On the other hand, significant correlation has been found for belts *II* and *III*, whose lower-latitude boundaries are around 40° at both hemispheres. A recent theoretical analysis [*Aharonson and Schorghofer*, 2006] suggests that the near-surface thermal conditions of current Mars allow the stable surface ice at latitudes ~40° and higher. Water ice is most likely to be stable in areas with favorable pole-looking slopes and high surface albedo. In this context, the presence of a correlation between near-IR and neutron albedo suggests that the fractional area with stable water ice is large enough to be observable from orbit poleward of 40°N and 40°S, and that the ice table is covered by a dry layer of regolith of *ETL*-type.

[15] On the other hand, according to neutron data, a water ice permafrost is known to exist in belt *IV* poleward of latitude 60°S, which does not display any significant correlation between near-IR and neutron albedo (Figure 2). The absence of a correlation in belt *IV* is the essential difference between the northern and southern permafrost provinces: the former corresponds to belt *II* with strong correlation at all latitudes. We conclude that water ice within belt *IV* must exist at different physical conditions from the ice in belts *II* and *III*. From the HEND neutron data we know [*Mitrofanov et al.*, 2004; *Litvak et al.*, 2006] that ice table in belt *IV* is covered by dry regolith with a thickness about 15–20 cm. The absence of a correlation between near-IR and neutron albedo indicates that that top layer within belt *IV* is physically different from the *ETL* within belts *II* and *III*. The surficial Dry Top Layer (DTL) may be out of equilibrium in the belt *IV* probably because dust storms rapidly change the thickness of dry layer or/and surface albedo for sunlight. One could expect that for the belt *IV* variation time of *DTL* is significantly shorter than the equilibrium timescale: the *ETL* within belt *IV* never has enough time to form.

3. Conclusions

[16] On the basis of joint analysis of near-IR radiometry from MOLA and neutron albedo from HEND, we conclude that there should be two different types of water ice permafrost on Mars. The first type lies in northern hemisphere poleward of 40°N and in the southern hemisphere between 40°S–60°S. This type of permafrost zone is covered by an *equilibrium top layer* (*ETL*), and the ice table currently exchanges with the atmosphere. The burial depth of permafrost in this type zone depends on the absorbed solar flux (cf. Figure 3). The second type of permafrost occurs in the southern hemisphere in the latitude belt 60°S–80°S. The ice table of this type of permafrost is out of equilibrium with the atmosphere, either because the *DTL* completely isolates it, or because the surface albedo changes too rapidly, probably due to dust storms, to achieve equilibrium.

[17] From the neutron and radiometry observations we have deduced an empirical relation (2) for the estimated thickness of the dry layer for the first type (*ETL*) of permafrost that has rather interesting practical applications. The present orbital neutron data has very poor spatial resolution (~300 km), while the map of near-IR albedo A_{1064} is known with sub-kilometer spatial resolution. Using the empirical relation (2) and the estimated average water ice content for 300-km surface blocks of the neutron map, we may estimate the burial depth for 1-km pixels within it. This procedure may be useful for estimating the shallow subsurface structure at candidate landing sites for the *Phoenix* mission, which is expected to land within the northern permafrost, and for assessment of landing sites of Mars Science Lander (*MSL*) which is planned to land at moderate latitudes (45°N–45°S).

References

Aharonson, O., and N. Schorghofer (2006), Subsurface ice on Mars with rough topography, *J. Geophys. Res.*, *111*, E11007, doi:10.1029/2005JE002636.

Bishop, J. L. (2005), Hydrated minerals on Mars, in *Water on Mars and Life*, edited by T. Tokano, chap. 4, pp. 65–97, Springer, New York.

Boynton, W. V., et al. (2002), Distribution of hydrogen in the near surface of Mars: Evidence for subsurface Iie deposits, *Science*, *297*, 81–85.

Feldman, W. C., et al. (2002), Global distribution of neutrons from Mars: Results from Mars Odyssey, *Science*, *297*, 75–78.

Litvak, M. L., I. G. Mitrofanov, A. S. Kozyrev, A. B. Sanin, V. I. Tretyakov, W. V. Boynton, N. J. Kelly, D. Hamara, C. Shinohara, and R. S. Saunders (2006), Comparison between polar regions of Mars from HEND/Odyssey data, *Icarus*, *180*, 23–37.

Mellon, M. T., and B. M. Jakosky (1995), The distribution and behavior of Martian ground ice during past and present epochs, *J. Geophys. Res.*, *100*, 11,781–11,799.

Mitrofanov, I. G., et al. (2002), Maps of subsurface hydrogen from the High Energy Neutron Detector, Mars Odyssey, *Science*, *297*, 78–81.

Mitrofanov, I. G., et al. (2003), CO_2 snow depth and subsurface water-ice abundance in the northern hemisphere of Mars, *Science*, *300*, 2081–2084.

Mitrofanov, I. G., M. L. Litvak, A. S. Kozyrev, A. B. Sanin, V. I. Tret'yakov, W. V. Boynton, C. Shinohara, D. Hamara, and R. S. Saunders (2004), Estimation of water content in Martian regolith from neutron measurements by HEND onboard 2001 Mars Odyssey, *Sol. Syst. Res.*, *38*(4), 253–257.

Schorghofer, N., and O. Aharonson (2005), Stability and exchange of subsurface ice on Mars, *J. Geophys. Res.*, *110*, E05003, doi:10.1029/2004JE002350.

Smith, D. E., et al. (2001), Mars Orbiter Laser Altimeter (MOLA): Experiment summary after the first year of global mapping of Mars, *J. Geophys. Res.*, *106*, 23,689–23,722.

Sun, X., G. A. Neumann, J. B. Abshire, and M. T. Zuber (2006), Mars 1064-nm spectral radiance measurements determined from the receiver noise response of the Mars Orbiter Laser Altimeter, *Appl. Opt.*, *45*, 3960–3971.

Zuber, M. T., D. E. Smith, S. C. Solomon, D. O. Muhleman, J. W. Head, J. B. Garvin, J. B. Abshire, and J. L. Bufton (1992), The Mars Observer Laser Altimeter investigation, *J. Geophys. Res.*, *97*, 7781–7798.

W. V. Boynton and D. Hamara, Lunar and Planetary Laboratory, University of Arizona, Tucson, AZ 85721, USA.

N. E. Demidov, A. S. Kozyrev, M. L. Litvak, I. G. Mitrofanov, A. B. Sanin, and V. I. Tretyakov, Institute for Space Research, Profsojuznaya st. 84/32, Moscow 117997, Russia. (imitrofa@space.ru)

D. A. Gilichinsky, Institute of Physical-Chemical and Biological Problems of Soil Science, Pushchino 142290, Russia.

R. D. Saunders, NASA Headquarters, Washington, DC 20514, USA.

D. E. Smith, Solar System Exploration Division, NASA Goddard Space Flight Center, Greenbelt, MD 20771, USA.

M. T. Zuber, Department of Earth, Atmospheric and Planetary Sciences, Massachusetts Institute of Technology, Cambridge, MA 02139-4307, USA.